Chemie der Erde 77 (2017) 477–486

Contents lists available at ScienceDirect

Chemie der Erde

journal homepage: www.elsevier.de/chemer

Isotope geochemistry of Mississippi Valley Type stratabound F-Ba-(Pb-Zn) ores of Hammam Zriba (Province of Zaghouan, NE Tunisia)

Nejib Jemmali[a,*], Emmanuel John M. Carranza[b,c,d], Balkiss Zemmel[a]

[a] Université de Gafsa, Faculté des Sciences, Département de Géologie, Sidi Ahmed Zarroug, 2112 Gafsa, Tunisia
[b] Economic Geology Research Centre, Department of Earth and Oceans, James Cook University, Townsville, Queensland, Australia
[c] Geological Sciences, School of Agricultural, Earth and Environmental Sciences, University of KwaZulu-Natal, South Africa
[d] Institute of Geosciences, State University of Campinas, Campinas, São Paulo, Brazil

ARTICLE INFO

Article history:
Received 11 September 2016
Received in revised form 14 June 2017
Accepted 5 July 2017
Editorial handling - J. Jacek Puziewicz

Keywords:
Hammam Zriba
Province of Zaghouan
Fluorite-barite
Stratabound mineralization
Isotope geochemistry

ABSTRACT

The Hammam Zriba F-Ba-(Zn-Pb) ore deposit in the Province of Zaghouan in north-eastern Tunisia is hosted in the shallow dipping unconformity between green marls with chalky biomicritic limestones of Campanian age and Uppermost Jurassic carbonates. The mineralization consists mainly of fluorite and barite with minor sphalerite and galena. Calcite is the main gangue mineral. Two types of Zn-Pb sulfides can be distinguished according to the geometry of the orebodies, i.e., lenticular or stratiform ores, intra-karstic fillings. Sulfur isotope compositions ($\delta^{34}S$) of barite range from 14.7 to 17.2‰, indicating that sulfur was derived from Triassic evaporites and the higher ones (19–25.7‰) are due to reservoir effect associated with thermo-chemical sulfate reduction (TSR) or bacterial sulfate reduction (BSR) under conditions of restricted sulfate supply. $\delta^{34}S$ of galena and sphalerite in lenticluar and intra-karstic orebodies range from −13.8 to 2.1‰, and could be explained by multiple sources of reduced sulfur: Triassic evaporites, diagenetic primary sulfides as well as sulfur from organic matter. Both TSR and BSR as potential contributors of sulfur are needed for sulfide precipitation. Lead isotope compositions of galena exhibit very similar: $^{206}Pb/^{204}Pb$ (18.858–18.876), $^{207}Pb/^{204}Pb$ (15.667–15.684), and $^{208}Pb/^{204}Pb$ (38.680–38.747) ratios, and plot between the upper crust and orogene average growth curves, reflecting involvement of a mixing and subsequent homogenization of Pb isotopic compositions of different source Pb reservoirs. The underlying Paleozoic basement rocks were the plausible source of metals. The economic ore (fluorite F1) mineralization was formed during the Eocene-Miocene compressional phase. During this deformation phase, deep-seated basinal brines have been circulated as hydrothermal fluids that have interacted with the Paleozoic rocks, thereby leaching metals, and have been channelized through subsidiary faults associated with the major regional NE–SW-trending deep-seated Zaghouan-Ressas fault. Hydrothermal fluids then migrated to the site of deposition where they got mixed with shallow, cooler, metal-depleted, TSR- and BSR-derived sulfur-rich fluids, which triggered the precipitation of the ores.

1. Introduction

The tectonic evolution of the Zaghouan-Ressas structural belt (ZRSB), which is situated in north-eastern Tunisia (Fig. 1), is mainly a consequence of the following major tectonic events (Morgan et al., 1998; de Lamotte et al., 2009). The Triassic-Early Jurassic period was characterized by the development of N–S trending normal faults and E–W trending transfer faults, which defined the eastern margin of a Jurassic carbonate platform. During the middle Jurassic – Early Cretaceous extensional period, the inherited E–W trending fault, which was controlled by major faults linked to the basement, continued to be active. This defined paleo-heights characterized by condensed sequences and elongated basins (Bouaziz et al., 2002) and the absence of the major part of Cretaceous rocks at Hammam Zriba, which are consistent with the persistence of the ZRSB at paleo-heights at that time (Morgan et al., 1998). The geodynamic context during the Late Cretaceous – Early Eocene was characterized by convergence, as expressed by NE–SW trending folds. The Late Eocene – Early Miocene compressive event was marked

* Corresponding author at: Faculté des Sciences de Gafsa, Sidi Ahmed Zarrouk, 2112 Gafsa, Tunisie.
E-mail address: nejib.jemmali@yahoo.fr (N. Jemmali).

http://dx.doi.org/10.1016/j.chemer.2017.07.003
0009-2819/

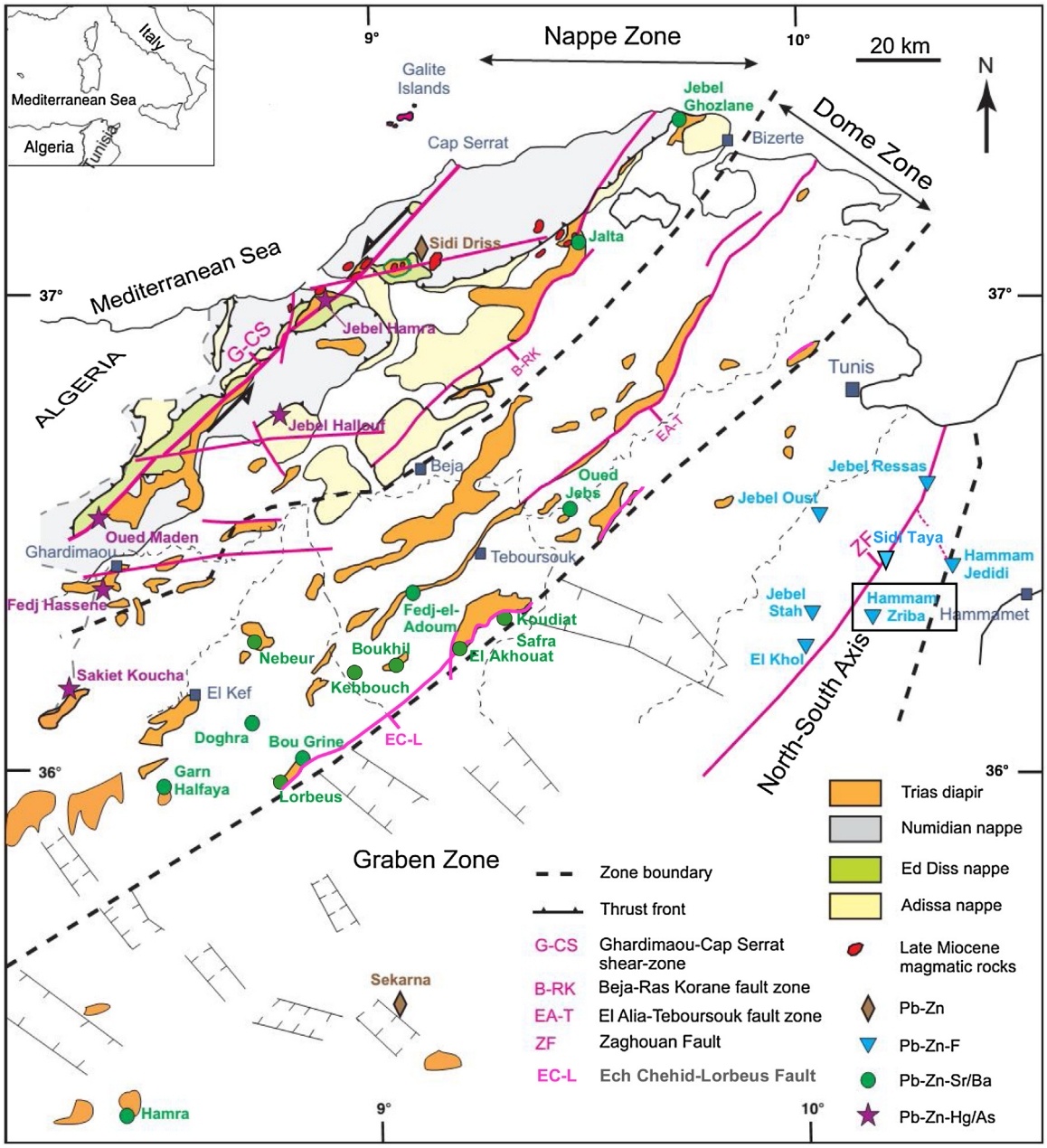

Fig. 1. Tectonic and metallogenic map of Northern Tunisia (adapted from Burrolet, 1991; Perthuisot, 1978; Jemmali et al., 2011; Decrée et al., 2016).

by an angular unconformity at the base of the Oligocene and the development of an Oligo–Miocene foreland basin. Contractional deformation of foreland basin sediments in the ZRSB occurred in Early Miocene (post-Tortonian, pre-Messinian), and that represented the main deformation responsible for the formation of the Atlas fold-thrust belt in Tunisia (Morgan et al., 1998).

Several economically significant sediment-hosted F-Ba-Sr-(Zn-Pb-Cu-Hg) deposits occur along the ZRSB (Fig. 1). Their mineralization is typically fluorite-rich and sulfide-poor, and shares characteristics with MVT deposits such as the carbonate nature of the host rocks, the basinal brine nature of fluids, the temperature of mineralizing fluids, the epigenetic character of mineralization, the crustal source of metals and no magmatism associated (Souissi et al., 1997, 2010, 2013; Jemmali et al., 2011a). The province of Zaghouan is one of the most important fluorite-producing regions in Tunisia. The deposits include the large Hammam Zriba F-Ba (Zn-Pb) deposit, Sidi Taya F-Pb (Zn-Ba-Sr) deposit, Jebel Mecella F-Zn-Pb deposit, Hammam Jedidi F-Ba (Zn-Pb) deposit, Jebel Stah F deposit, Jebel Oust F-Cu-Hg deposit, and the Jebel Ressas Pb-Zn (Fe) deposit (Fig. 1). Most of these deposits are hosted in the Lower Liassic or Upper Jurassic massive limestones and the overlying Upper Sinemurian-Carixian condensed limestones and Campanian marls. Because they have no direct relationship with magmatism they are considered to have formed from basinal brines that were mobilized during the Alpine orogeny (Souissi et al., 1997; Jemmali et al., 2011a).

Fluid inclusion measurements in fluorite from Hammam Zriba indicate that the ore-forming fluids were hot (>100° ± 20 °C) and saline (>13 wt% NaCl equiv) basin-derived brines (Bouhlel et al., 1988). These brines acquired high salinities and high molar ratios (Ca/Na, SO_4/Cl, Cl/Na), except for lower Mg/Na ratio, at depth from the leaching of the Triassic evaporites by ascending hot fluids (Souissi et al., 1997). The measured homogenization temperatures (110–185 °C; Bouhlel et al., 1988) combined with the thickness

of the overburden, which never exceeded 2100 m at the time of ore deposition, imply a highly anomalous geothermal gradient that range between 50 and 70 °C/km. Consequently, the reservoir of the fluids should be 3500–5000 m deep below the ore bearing layers (Souissi et al., 1997).

In the current study, fluorite-bearing Zn-Pb ores from Hammam Zriba have been investigated for their sulfur and lead isotopes composition to elucidate the source of reduced sulfur, mechanisms of ore deposition and possible age of mineralization.

2. Hammam Zriba deposit geology

The Hammam Zriba F-Ba-Zn-Pb deposit is located about 8 km SE of Zaghouan town and 60 km south of Tunis. It is situated in a horst structure, with varying thickness (0.3–1 km) and NNW–SSE strike over ~3 km (Fig. 2). This horst has formed during late Jurassic as an emerged block bounded by major faults that were remobilized later during various deformation stages (Melki and Zargouni, 1991) and limited mainly by two normal faults (Gharbi et al., 1981): one (F1) striking N135–145°E and dipping 50–70°NE and another (F2) striking N130–150°E and dipping 50–70°SW. A N160–N180 trending fault in the Portlandian lithofacies has controlled the paleo-morphological framework of the uppermost part of the Portlandian massive facies. The overlying Campanian unit exhibits onlap structures that rest on the irregular eroded karstified and mineralized surface, which forms a screen surface for the upward channelization of fluids and subsequent mineral deposit formation in karst and graben (Melki and Zargouni, 1991). Rocks in the Hammam Zriba mine are intensely fractured at different scales on the surface and in the subsurface (Fig. 2). The stratigraphy comprises a series of sedimentary rocks from the Portlandian to the Eocene with a hiatus from the Berriasian to the middle-Campanian, corresponding to an emersion period (Thibieroz, 1974, 1976) (Figs. 2 and 3). The Portlandian series consists of massive, thick, biomicritic and grey limestones. The Campanian comprises green marls with chalky biomicritic limestones. The bottom of the Campanian series contains some thin and discontinuous black phosphatic-shale levels. The Maastrichtian and Paleocene series are composed of beige limestones and interbedded grey and green marls respectively. The Eocene is dominated by grey, thick, phosphate-bearing limestones beds and green marls.

The Hammam Zriba has been classified by Souissi et al. (1997) as a typical MVT deposit. Underground mining of this deposit was operated from 1967 to 1992, when more than 4 Mt of ore grading 25% fluorite (CaF_2), 1–2% Pb + Zn has been produced (Maghreb Minerals, 2008).

3. Sampling and analytical methods

A total of 38 representative samples from sulfide (galena: n = 10; sphalerite: n = 5) and sulfate (barite: n = 23) minerals were collected from mine workings and outcrops of lenticular and intrakarstic ores. Mineral separates of galena, sphalerite and barite were prepared for conventional sulfur isotope analysis by careful hand-picking under a binocular microscope, and were analyzed at the laboratory of the Institute of Mineralogy and Geochemistry of the University of Lausanne (Switzerland) using a Carlo Erba 1100 elemental analyzer (EA) connected to a Thermo Fisher Delta S isotope ratio mass spectrometer (IRMS) that was operated in the continuous He flow mode via a Conflo III split interface (EA-IRMS). The sulfur isotope compositions are reported as per mil (‰) deviations relative to the Canyon Diabolo troilite (V-CDT) standard. The overall analytical reproducibility of the EA-IRMS analyses, assessed by replicate analyses of two laboratory standards (barium sulfate, with a working $\delta^{34}S$ value of +12.5‰; pyrite E, −7.0‰) is better than ±0.2‰ (1 SD). The accuracy of the $\delta^{34}S$ analyses was checked periodically by analyses of the international reference materials IAEA-S-2 silver sulfides (+22.7 ± 0.2‰, values from IAEA-Catalogue and Documents) and NBS-123 sphalerite (+17.09 ± 0.31‰, value from NIST-Catalogue and Documents).

For Pb isotope measurements, 2–3 mg of galena sample was dissolved using ultrapure (double distilled) HCl. The Pb isotope compositions were analyzed using a multi-collector inductively coupled plasma mass spectrometer instrument within the

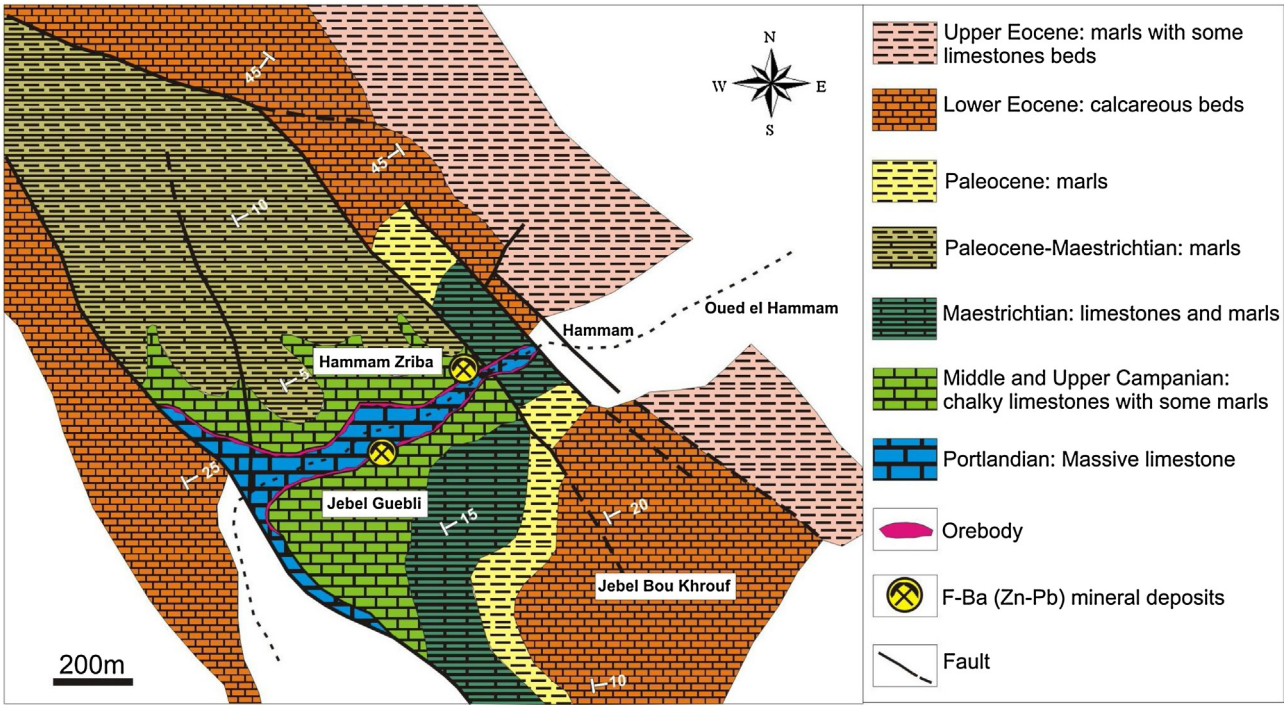

Fig. 2. Geologic map of the Hammam Zriba F-Ba-Sr (Zn-Pb) deposit, showing major faults and distribution of ore bodies (adapted from Melki and Zargouni, 1991).

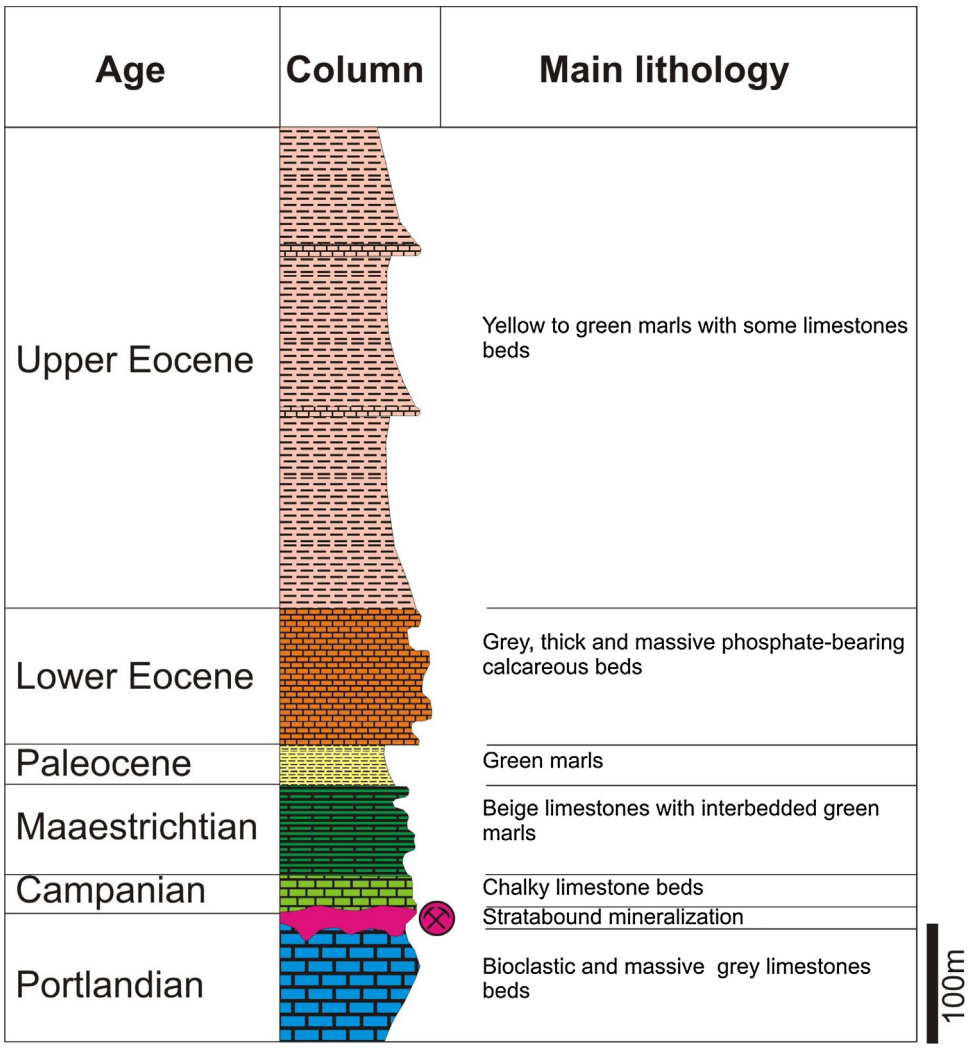

Fig. 3. Main lithostratigraphic column of the Hammam Zriba deposit (adapted from Melki and Zargouni, 1991).

Radiogenic Isotope facility at the University of Bern (Switzerland). Sample aliquots were subsequently mixed with ~1.5 ml of a 2% HNO_3 solution spiked with the NIST SRM 997 Thallium standard (2.5 ppb), and aspirated (~100 μl/min) into the ICP source using an Apex^{TM} desolvating nebulizer (Nu Instruments Ltd). Simultaneous measurements of all the Pb and Tl isotopes, and ^{202}Hg ion signal were achieved by using seven Faraday collectors. The ^{205}Tl/^{203}Tl ratio was measured to correct for instrumental mass bias (exponential law; ^{205}Tl/^{203}Tl = 2.4262). Upon sample introduction, data acquisition consisted of 2 half-mass unit baseline measurements prior to each integration block, and 3 blocks of 20 scans (10 s integration each) for isotope ratio analysis. ^{204}Hg interference (on ^{204}Pb) was monitored and corrected using ^{202}Hg. At the beginning of the analytical session, a 25 ppb solution of the NIST SRM 981 Pb standard, which was also spiked with the NIST SRM 997 Tl standard (1.25 ppb), was analyzed. The external reproducibility of individual analytical sessions was ca. 1×10^{-4}.

4. Results

4.1. Ore petrography

The mineralization is structurally- and lithologically-controlled and hosted in the shallow dipping unconformity between Campanian green marls with chalky biomicritic limestones and Jurassic reef limestones (Fig. 2). It consists of fluorite and barite as the dominant ore minerals associated with accessory celestite and some minor sulfides, including both sphalerite and galena. Dill et al. (2014) also reported the presence of minor minerals such as mimetite (zincian), pyromorphite, smithsonite, and traces of hemimorphite. Calcite and quartz are the gangue minerals.

The synthesis of our detailed examination of hand specimens of ore samples (Fig. 4) with the studies of Thibieroz (1974) and Bouhlel et al. (1988) reveals the following fluorite types:

- fluorite 1, the main economic ore, is a banded ore made of coarse-grained fluorite alternating with bands of spherulitic barite 1 and quartz, associated with galena 1 and sphalerite 1 in the black siliceous facies (diagenetic type mineralization (Mo) according to Bouhlel et al. (1985)) and bands of white fibrous barite 2, which contains galena 2 crystals;
- fluorite 2, which is made of large crystals within karstic pockets cutting over the fluorite 1 and associated with galena 2 and sphalerite 2 and massive barite 3; and
- fluorite 3 consisting of large cubic crystals within geodes in the banded ore and the karstic pockets.

Three types of ores can be distinguished according to the geometry of the orebodies:

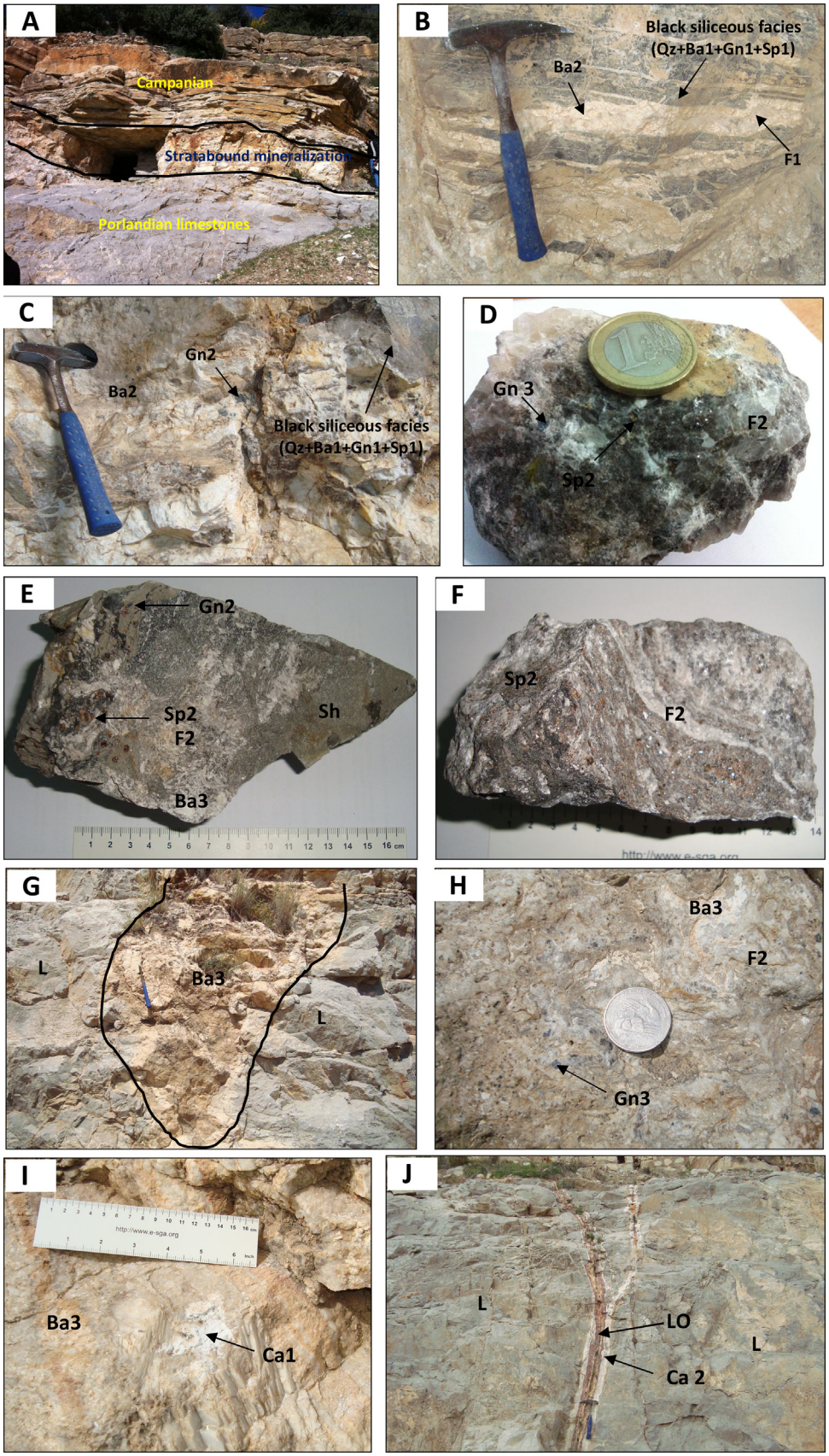

Fig. 4. Appearance of representative field and hand specimens of all types of Hammam Zriba F-Ba- (Pb-Zn) orebodies occurring within the unconformity between Portlandian and Upper Cretaceous rocks. A: stratabound mineralization along the unconformity between Portlandian and Upper Cretaceous rocks. B: Banded ore with fluorite 1 (F1), black siliceous facies "Type M0" with spherulitic barite 1 (Ba1), authigenic quartz and diagenetic sulfides (galena and sphalerite) and barite 2 (Ba2) in lenticluar orebody. C: white fibrous barite 2 (Ba2) with cubic crystals of galena 2 (Gn2) in lenticular orebody. D: fluorite 2 (F2) with fine-grained galena 3 (Gn3) and brown sphalerite (Sp2) in intra-karstic orebody. E: Cretaceous black shales (Sh) with fluorite 2 (F2), fibrous barite 3 (Ba3) associated with fine grained galena 2 (Gn2) and brown sphalerite (sp2) in intra-karstic orebody. F: fluorite 2 (F2) associated with brown sphalerite (Sp2) in intra-karstic orebody. G: intra-karstic ore with fibrous barite 3 (Ba3), hosted by Portlandian limestones (L). H: coarse-grained galena 3 (Gn3) associated with barite 3 (Ba3) and fluorite 2 (F2) in intra-karstic ore. I: calcite rhombohedra (Ca1) associated to barite 3 (Ba3) in intra-karstic ore. J: veins in Portlandian limestones filled with Calcite 2 (Ca2) and limestone Onyx (LO).

Table 1
Mineral paragenetic sequence in the Hammam Zriba deposit.

Processes	Diagenesis	Epigenetic replacement Hydraulic fracturing Karstification Fracturation	Oxidation
Mineral	Pre-ore stage	Hydrothermal ore stage	Post-ore stage
Quartz (Qz)	Qz		
Pyrite (Py)	Py		
Sphalerite (Sp)	Sp1	Sp2	
Galena (Gn)	Gn1	Gn2, Gn3	
Barite (Ba)	Ba1	Ba2, Ba3	
Fluorite (F)		F1, F2, F3	
Calcite (Ca)		Ca1, Ca2	
Smithsonite (Sm)			Sm
Hemimorphite (Hm)			Hm
Pyromorphite (Pr)			Pr

(i) lenticular or stratabound ores are the most important and widespread, in close association with sub-horizontal hydraulic fractures. This type of mineralization occurs between the Portlandian (wall) and the Campanian (roof) (Fig. 4A), and exhibits banded texture composed of black siliceous facies (Fig. 4B) and white fibrous barite 2 (Ba2) alternating with fluorite 1 (F1). Epigenetic galena 2, with cubic crystals (Gn2), was found disseminated in barite 2 (Ba2) (Fig. 4C).
(ii) intra-karstic ores in the Portlandian limestones correspond to fillings of cavities, which are not parallel to the bedding, and consist of fluorite 2 (F2) (Fig. 4E, F, H) associated with rare, fine galena 3 (Gn3) and sphalerite crystals (Sp2) (Fig. 4D, E, F, H); massive white barite 3 (Ba3) (Fig. 4E, G, H, I) and large rhombohedra of calcite 1 (Ca1) crystals (Fig. 4J);
(iii) vein fillings in fractures cutting the Portlandian limestones, with calcite 2 (Ca2) (Fig. 4K, L) and limestone onyx (LO) (Fig. 4K, L).

Based on the textural, mineralogical associations observed within the deposit and based on the previous works of Bouhlel et al. (1988), mineralization has been classified into three stages (Table 1): (1) pre-ore stage (diagenetic period) consisting of quartz, galena 1, sphalerite 1, barite 1 and pyrite associated with organic matter (Type Mo); (2) hydrothermal ore stage composed of four sub-stages: sub-stage 2a disseminated galenas 2 and 3 and sphalerite 2, sub-stage 2b barites 2 and 3, sub-stage 2c fluorites 1, 2 and 3, and sub-stage 2d calcites 1 and 2; and (3) post-ore stage composed of secondary minerals (smithsonite, hemimorphite and pyromorphite).

4.2. Sulfur isotope compositions

The $\delta^{34}S$ data obtained in this study (Table 2) represent various lenticular and intra-karstic ores, and sulfur-mineral assemblages of the Hammam Zriba ore deposit. The $\delta^{34}S$ data range from −13.8 to −1.4‰ for galenas 1 and 2, 1.7–2.1‰ for sphalerite, and 14.8–25.7‰ for all barites (Fig. 5).

For the lenticluar ore, the $\delta^{34}S$ values of galena 2 range from −13.8 to −11.2‰ (average = −12.73‰). The barite 1 has $\delta^{34}S$ values ranging from 15.4 to 16.9‰ (average = 16.4‰), which are close to the average $\delta^{34}S$ value of Triassic evaporates of Jebel Ressas (16.4‰; Jemmali et al., 2011a). The barite 2 is more enriched in ^{34}S, with $\delta^{34}S$ values between from 19 to 25.7‰ with average of 22.35‰.

For the intra-karstic ore, the $\delta^{34}S$ values range from −2.6 to 2.1‰. Disseminated galena 3 and sphalerite 2 associated with the black shales show narrow ranges of $\delta^{34}S$ values (−2.6 to −1.4‰ with an average −2.17 and 1.7–2.1‰ with an average 1.92‰, respectively). The associated barite 3 has $\delta^{34}S$ values ranging from 14.6 to 17.2‰ (average = 15.6‰). This mean $\delta^{34}S$ of barite 3 is close to the average $\delta^{34}S$ a value of Triassic evaporates of Jebel Ressas (Jemmali et al., 2011a).

Table 2
Sulfur isotope compositions of sulfides (galena and sphalerite) and sulfate (barite) from the Hammam Zriba deposit, and gypsum from Jebel Ressas (Jemmali et al., 2011a).

Mineral phase	Mineralization type	$\delta^{34}S$ (‰, VCDT)
Galena 2	Lenticular	−11.2
		−13.8
		−13.2
Barite 1		15.4
		16.8
		16.9
		16.4
		16.1
		16.3
		16.9
		16.3
		16.4
Barite 2		19.0
		19.1
		19.3
		25.4
		25.6
		25.7
Galena 3	intrakarstic	−2.5
		−2.4
		−2.5
		−2.6
		−1.5
		−1.4
		−2.3
Sphalerite 2		2.0
		2.1
		1.7
		1.8
		2.0
Barite 3		15.9
		16.4
		16.5
		14.7
		14.8
		17.2
		14.6
		14.7

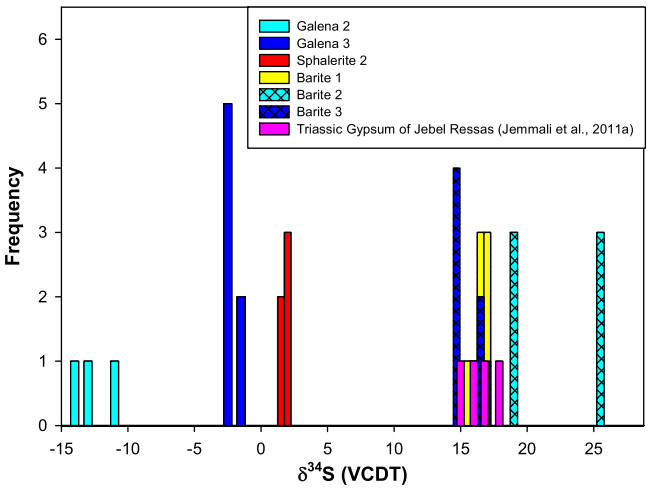

Fig. 5. Frequency distribution of $\delta^{34}S$ values for mineral separates of sphalerite 2, galenas 1 and 2, all types of barites from the Hammam Zriba deposit. Also shown for comparison is the sulfur isotope range for Triassic evaporates at Jebel Ressas (Jemmali et al., 2011a).

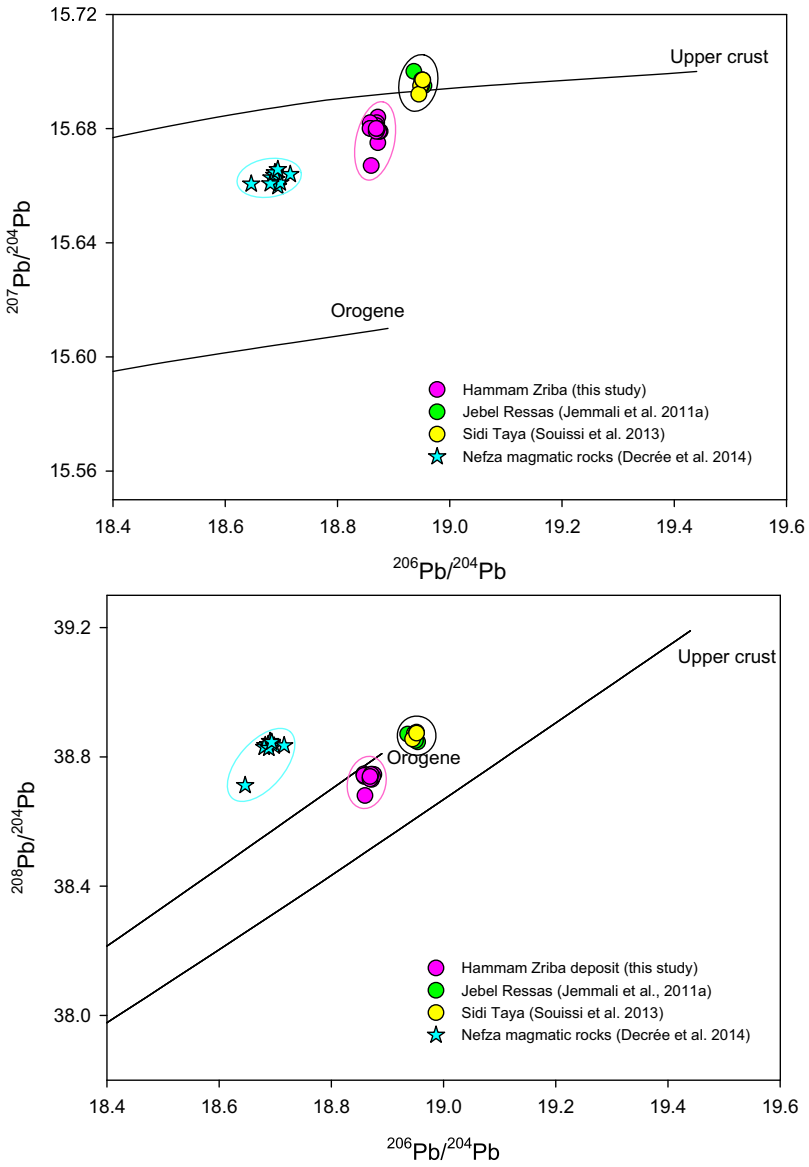

Fig. 6. Plots of lead isotope compositions of galena from the Hammam Zriba deposit, including analyses of Jebel Ressas, Sidi Taya galenas from Jemmali et al. (2011b) and Souissi et al. (2013), and analyses of Nefza magmatic rocks from Decrée et al. (2014). Evolution curves for upper crust and orogene from Zartman and Doe (1981) are shown for reference.

4.3. Lead isotope compositions

The results of lead isotope analyses of the Hammam Zriba galena samples are given in Table 3 and plotted on Fig. 6. For comparison, the lead isotopic values of galena from other Tunisian carbonate-hosted deposits studied by Jemmali et al. (2011a) and Souissi et al. (2013) and from Nefza magmatic rocks studied by Decrée et al. (2014) are also shown. Lead from the Hammam Zriba deposit is isotopically homogeneous and show fairly uniform $^{206}Pb/^{204}Pb$ (18.858–18.876), $^{207}Pb/^{204}Pb$ (15.667–15.684), and $^{208}Pb/^{204}Pb$ (38.680–38.747) ratios (Table 2; Fig. 6), which clearly indicate a crustal source of lead.

Table 3
Ratios of Pb isotope compositions in galena from the Hammam Zriba deposit.

Mineralization type	$^{206}Pb/^{204}Pb$	$^{207}Pb/^{204}Pb$	$^{208}Pb/^{204}Pb$
Lenticular (galena 2)	18.872	15.684	38.746
	18.870	15.682	38.742
	18.869	15.681	38.740
	18.860	15.667	38.680
	18.872	15.675	38.730
	18.876	15.679	38.745
	18.874	15.679	38.739
Intrakarstic (galena 3)	18.858	15.682	38.747
	18.859	15.680	38.739
	18.858	15.680	38.742
	18.869	15.679	38.731
	18.871	15.680	38.745
	18.869	15.680	38.739

5. Discussion

5.1. Sources of sulfate

The $\delta^{34}S$ values of barite in Hammam Zriba are considerably variable. The $\delta^{34}S$ values of barites 1 and 2 from lenticular ores and barite 3 from intra-karstic ore are mostly in the range between 14.6–25.7‰ (Table 2). Two populations may be identified (Fig. 5). One population (barites 1 and 3) corresponds to $\delta^{34}S$ values in the

range between 14.6 and 17.2‰ with an average of 16‰; the second population (barite 2) includes only six barite samples with substantially higher $\delta^{34}S$ values in the range between 19 and 25.7‰ with an average of 22.35‰. The $\delta^{34}S$ average values of barites from the population 1 overlaps with the typical composition of Triassic evaporitic rocks of Jebel Ressas (Jemmali et al., 2011a), which show a well-defined and narrow range of $\delta^{34}S$ values from 15 to 17.9‰ (Fig. 5). This suggests that the majority of dissolved sulfate in the hydrothermal fluids that formed the base metal mineralization in Hammam Zriba was derived from groundwater that had interacted with Triassic evaporites. The second population includes barite samples with S isotope ratios higher than the first population values and different from those of Triassic evaporates.

The repeated cycles of Triassic gypsum dissolution/reprecipitation by meteoric waters may have generated residual brines that were slightly depleted in ^{34}S (Thode and Monster, 1965), with high Sr-Ba/Ca, as necessary for Sr-Barite mineralization (Hanor, 2000). During the crystallization of sulfates the residual fluid was not enriched, but was slightly depleted in ^{34}S; thus, the isotopic shift in the second population of barite indicates that it did not precipitate from residual brines. Considering the epigenetic character of the Hammam Zriba deposit, the formation of Ba-Sr and Pb-Zn-rich brines was likely coupled to a mechanism that simultaneously led to a significant fractionation of the S isotopes (Dill et al., 2009). The high $\delta^{34}S$ values can be due to reservoir effect associated with thermo-chemical sulfate reduction (TSR) or bacterial sulfate reduction (BSR) under conditions of restricted sulfate supply (Dill et al., 2009).

5.2. Source (s) of sulfur

The most important characteristic of the lenticular ores at Hammam Zriba is that they have substantially more negative $\delta^{34}S$ values for galena in the range between −13.8 and −11.2‰ compared to the intra-karstic ores, which have $\delta^{34}S$ values for galena that range between −2.6 and −1.4‰, and positive $\delta^{34}S$ values for sphalerite in the range between 1.7 and 2.1‰ (Table 2; Fig. 5). The differences of $\delta^{34}S$ values of galenas in lenticular and intra-karstic ores could be explained by two processes: (1) multiple sources of sulfur and (2) a single source of sulfur that evolved over time.

The most likely sources of reduced sulfur for the sulfide phases is Triassic evaporites, which were suggested as the likely source of sulfur in the Zaghouan district (Jemmali et al., 2011a; Souissi et al., 2013) and other carbonate-hosted Pb-Zn deposits in the Nappe and Dome zones (Jemmali et al., 2011b, 2013a, 2013b). The observed isotopic compositions for sulfide minerals at Hammam Zriba may be explained by reduction of these sulfate sources through TSR and/or BSR.

It is well established that BSR takes place at 60–80 °C, and may occur at temperatures as high as 110 °C (Jorgensen et al., 1992). TSR takes place at higher temperatures (mainly 80–130 °C), though it becomes more active at even higher temperatures. The average temperature of fluorite precipitation of 100–185 °C overlaps to some extent with both BSR and TSR regimes. The temperature deduced from galena-sphalerite pair is ~128 °C using the equation of Grootenboer and Schwarcz (1969), which rather falls into the TSR regime. Moreover, TSR causes isotopic fractionation from ~0 to ~20 per mil (Kiyosu and Krouse, 1990; Machel et al., 1995), whereas BSR mechanism induces isotopic fractionation of ~40 per mil. The calculated isotopic fractionation range of 14.5–29‰ falls into the range of both regimes. Considering the temperature range and the negative values recorded in galena (up to −13.8‰), it is wise to consider both mechanisms (TSR and BSR) as potential contributors of sulfur needed for sulfide precipitation.

Mixing of TSR- and BSR-derived sulfur may account for the bulk isotopic sulfur composition. In fact, the sulfides in the Zaghouan province display negative values (up to −13.8‰) as well as very positive values in other similar ore deposits (up to +11.4‰; cf. Souissi et al., 2013). In this context, the very negative $\delta^{34}S$ values of galena 2 (average = −12.73‰) compared to that of galena 3 (average = −2.17‰) recorded in Hammam Zriba may indicate an increase of light sulfur from (i) mainly BSR-derived sulfur and to some extent (ii) organic sulfur, and/or diagenetic sulfides ($\delta^{34}S$ <−2.36‰; Bouhlel, 1993) in the dark siliceous facies associated with organic matter. The proportion of light sulfur and thus the superficial, depleted metal, bacteriologically-rich derived sulfur fluid, became more pronounced in the early stage (galena 2).

Following the multi-sulfur source hypothesis, not only TSR- and BSR-derived sulfur but also organic sulfur is considered as local source of sulfur though probably minor. The occurrence of oil fluid inclusions in all type of fluorites of Hammam Zriba (cf. Bouhlel et al., 1988) could indicate the contribution of organically bonded sulfur. In regard to this organically bonded sulfur and given the fact that the ore is associated with black shales, thermal cracking of organic matter (e.g., presence of hydrocarbon in fluid inclusion) can be considered as a possible local source of sulfur. The organic sulfur and diagenetic sulfides along with BSR could have lowered the sulfur isotopic composition of the epigenetic sulfides. The hydrocarbons observed in fluorite inclusions may indicate transport from a deeper mature source rock.

5.3. Sources of metals and age of mineralization

On conventional uranogenic and thorogenic plots (Fig. 6), data for most of the analyzed samples fall between the upper crustal and orogen model curves of Zartman and Doe (1981). The tight linear clustering of Pb isotope data for the galena ores may reflect involvement of mixing and subsequent homogenization of Pb isotopic composition of different source Pb reservoirs that would also explain the uniform isotopic values (Fig. 6).

The lead isotope composition data suggest that the lead in the Hammam Zriba deposit was derived from a different source than the lead in other Tunisian carbonate-hosted deposits and in the Nefza magmatic rocks, and has been interpreted to probably indicate regional differences in the composition of the underlying sediments, which probably include the Paleozoic basement (Jemmali et al., 2011a; Souissi et al., 2010; Souissi et al., 2013). The Pb isotope ratios of galena from Jebel Ressas and Sidi Taya deposits in the Zaghouan district are markedly higher and different than those from the Hammam Zriba deposit (Fig. 6), and are enriched in radiogenic lead indicating that the former were derived from a source enriched in both U and Th. The geographic position of the deposits was closely related to this variation and the differences in lead isotopic composition may reflect the spatial dissimilarity of involved crustal rocks (Jeong et al., 2012). This crustal source provenance is supported by strontium isotope data from minerals associated with the ore deposits in the Zaghouan Distric (i.e., Sidi Taya, Hammam Jedidi, Oued M'tak and Jebel Oust) (Souissi et al., 2013), which could have been sourced from connate waters trapped in the Paleozoic sedimentary column. Based on the data presented above, the Paleozoic seems to be the dominant source.

Geological field observations, textural crosscutting and paragenetic sequence, supported by fluid inclusions show the existence of three chronologically distinct stages of mineralization. Mineralization with fluorite types are epigenetic and formed after the lithification and dissolution of the Portlandian limestone host rocks, and are structurally-controlled due to the presence of N070–090 and N160–N180 trending faults (Melki and Zargouni, 1991). Thus, their emplacement postdates the Upper Jurassic (i.e., Portlandian). According to Melki and Zargouni (1991), the horst structure of Hammam Zriba has formed during the Late Jurassic as an emerged block bounded by major fault that was re-activated during var-

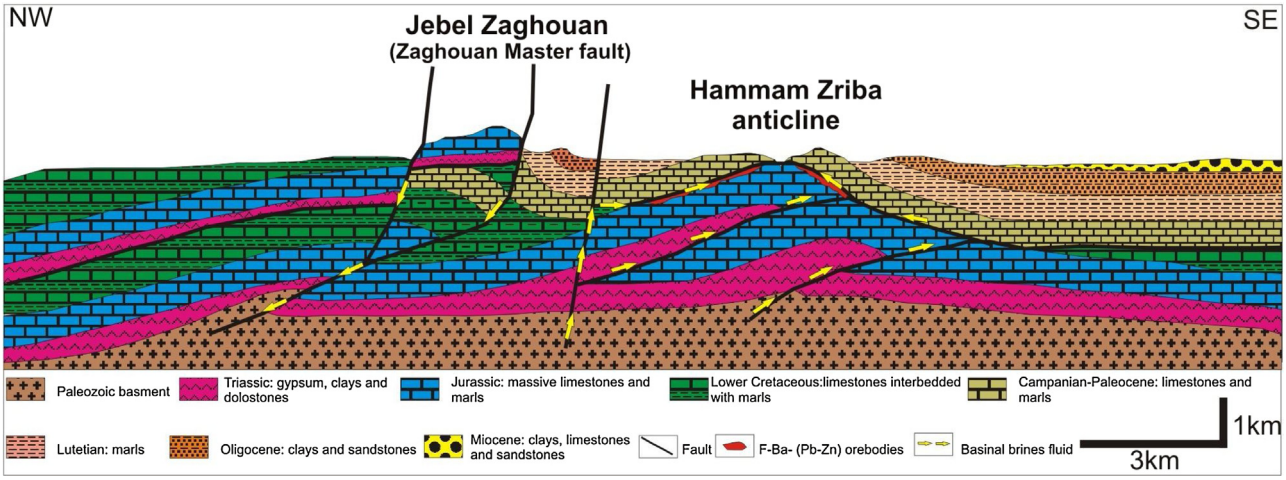

Fig. 7. Schematic proposed genetic model of the Hammam Zriba F-Ba- (Pb-Zn) ore deposit (adapted and modified based on present-day cross section of Jebel Zaghouan-Zriba from Morgan et al., 1998).

ious later tectonic events. The ultimate last phase in which the horst took the final form was the Tortonian period, which caused the mineral deposition (Melki and Zargouni, 1991). Furthermore, based on Sr isotope ages that range between 28 and 19 Ma, Dill et al. (2014) attributed the Tunisian salt-related deposits to the Chattian-Burdigalian age. Moreover, in the area of Oued M'Tak, the youngest rock series hosting F-(Zn-Pb) deposit is Miocene (Burdigalian) in age. All these arguments strongly suggest an Upper/Late Miocene age for the mineralization of Hammam Zriba deposit. The same age was suggested for other Tunisian Pb-Zn deposits (Decrée et al., 2008; Jemmali et al., 2011a, 2011b, 2013b; Souissi et al., 2013; Jemmali et al., 2014).

5.4. Proposed genetic model

Based on the geological, mineralogical and geochemical relationships discussed above, and published literature dealing with Hammam Zriba as cited in the discussion above, a proposed genetic model is postulated as follows.

At Hammam Zriba, anticlines are interpreted as fault-inversion folds that seem to have occurred during the late Eocene – early Miocene (Frizon de Lamotte et al., 2000), formed in normal sequence on the external side of the ZRSB. Flow of Triassic strata into the cores of these folds may have been assisted by tectonic loading during fault inversion along the ZRSB. Subsequently, structures in the ZRSB were dissected by NE–SW trending faults that propagated through the post-rift sequence during post-Miocene reactivation of syn-rift extensional faults. These faults were linked to extension in NW–SE trending graben that cut the ZRSB (Morgan et al., 1998). The Eocene–Miocene compressional phase "Alpine orogeny" caused the development of the foreland basin (Morgan et al., 1998). The generated topographic gradient induced the circulation of deep-seated basinal brines as hydrothermal fluids, as indicated by fluid inclusion temperatures of fluorites which are predominantly in the 100–185 °C range (Bouhlel et al., 1988), and the hydrothermal fluids acquired their salinity mainly from Triassic evaporates. The deep-seated basinal brines probably interacted with the basement rocks, thereby leaching metals, and were channelized through secondary faults associated with the ZRSB major regional NE–SW-trending deep-seated fault. Alternatively, the deep-seated, hot fluids migrated to the site of deposition where they got mixed with shallow, cooler, metal-depleted, TSR- and BSR-derived sulfur-rich fluid, which triggered the precipitation of the ores (Fig. 7). This mixing model is supported by wall-rock silicification, which indicates that hot fluids underwent conductive cooling as they encountered carbonate host rocks (Fournier, 1985; Rddad and Bouhlel, 2016), as well as by the temperature fluctuations recorded in fluorite. The lower part of the Campanian consists of marls and black shales, which acted as an impermeable barrier of the fluid circulation.

The proposed ore genesis model, which involves the interaction between basement-derived ore fluids and shallower H_2S-rich fluids, has similarities to numerous MVT ore deposits worldwide (e.g., Pine Point, Canada (Rhodes et al., 1984), Ozarks, USA (Leach, 1994; Souissi et al., 2007), Touissit-Bou Beker district, Moroccan-Algerian confines (Bouabdellah et al., 2012), Jebel Ressas, Tunisia (Jemmali et al., 2011a), and Bou Dahar, Morocco (Rddad and Bouhlel, 2016)).

6. Conclusions

The study of sulfur and lead isotope geochemistry of sulfide minerals allowed to constrain the genesis of sulfur and metals and the timing of fluorite-bearing Zn-Pb mineralization at Hammam Zriba, which occurs as lenticular (or stratiform) and intra-karstic ores in the shallow dipping unconformity between Campanian and Upper Jurassic carbonates. The following conclusions are reached:

(i) Ore mineral assemblage consists of fluorite and barite associated with minor sulfides, including sphalerite and galena. Calcite and quartz are the gangue minerals.
(ii) The $\delta^{34}S$ values of barite are much close to the $\delta^{34}S$ of Triassic evaporates. The $\delta^{34}S$ values of galena and sphalerite minerals indicate that the deposition of sulfides has resulted from mixing of TSR- and BSR-derived sulfur. The most likely sources of reduced sulfur for the sulfide phases are Triassic evaporites, and locally diagenetic sulfides and organic sulfur.
(iii) The Pb isotope compositions of galena have homogenous $^{206}Pb/^{204}Pb$ (18.858–18.876), $^{207}Pb/^{204}Pb$ (15.667–15.684), and $^{208}Pb/^{204}Pb$ (38.680–38.747) ratios, which suggest mixing and subsequent homogenization of Pb isotopic composition of different source Pb reservoirs: deep-sourced metal-rich brines from the underlying crustal rocks, possibly the Paleozoic basement.
(iv) The mineralization of Hammam Zriba deposit has likely an upper or late Miocene age.

Acknowledgements

We thank Professor Fouad Souissi (Faculty of Sciences of Tunis) for his assistance and discussion about the metallogeny of Hammam Zriba. We are grateful to Professor Larbi Rddad of the City University of New York and the anonymous reviewers for their comments, and to Associate Editor Jacek Puziewicz for expert handling of our paper.

References

Bouabdellah, M., Sangster, D.F., Leach, D.L., Rown, A.C., Johnson, C.A., Emsbo, P., 2012. Genesis of the Touissit-Bou Beker Mississippi Valley-Type District (Morocco–Algeria) and its relationship to the Africa Europe collision. Econ. Geol. 107, 117–146.

Bouaziz, S., Barrier, E., Soussi, M., Turki, M.M., Zouari, H., 2002. Tectonic evolution of the northern African margin in Tunisia from paleostress data and sedimentary record. Tectonophysics 357 (1), 227–253.

Bouhlel, S., Fortuné, J.P., Guilhaumou, N., Touray, J.C., 1988. Les minéralisations stratiformes à F-Ba de Hammam Zriba, Jebel Guébli (Tunisie nord orientale): l'apport des études d'inclusions fluides à la modélisation génétique. Miner. Deposita 23 (3), 166–173.

Bouhlel, S., 1993. Gîtologie, mineralogie et essai de modélisation des mineralisations a F-Ba-Sr-Pb-Zn-(S) associees aux carbonates (Jurassiques et Cretaces) et aux diapirs triasiques: Gisements de Stah-Kohol, Zriba-Guebli, Bou Jabeur et Fej lahdoum (Tunisie septentrionale). Thèse de doctorat. Faculté des Sciences de Tunis (303p).

Burrolet, P.F., 1991. Structures and tectonics of Tunisia. Tectonophysics 195, 359–369.

Decrée, S., Marignac, C., De Putter, T., Deloule, E., Liégeois, J.P., Demaiffe, D., 2008. Pb-Zn mineralization in a Miocene regional extensional context: the case of the Sidi Driss and the Douahria ore deposits (Nefza mining district, northern Tunisia). Ore Geol. Rev. 34, 285–303.

Decrée, S., Marignac, C., Liégeois, J.P., Yans, J., Abdallah, R.B., Demaiffe, D., 2014. Miocene magmatic evolution in the Nefza district (Northern Tunisia) and its relationship with the genesis of polymetallic mineralizations. Lithos 192, 240–258.

Dill, H.G., Henjes-Kunst, F., Berner, Z., Stüben, D., 2009. Miocene diagenetic and epigenetic strontium mineralization in calcareous series from Cyprus and the Arabian Gulf. Metallogenic perspective on sub- and suprasalt redox-controlled base metal deposits. J. Asian Earth Sci. 34, 557–576.

Dill, H.G., Nolte, N., Hansen, B.T., 2014. Lithology, mineralogy and geochemical characterizations of sediment-hosted Sr-F deposits in the eastern Neo-Tethyan region-With special reference to evaporation and halokinesis in Tunisia. J. Afr. Earth. Sci. 92, 76–96.

Decrée, S., Marignac, C., Abidi, R., Jemmali, N., Deloule, E., Souissi, F., 2016. Tectonomagmatic Context of Sedex Pb–Zn and Polymetallic Ore Deposits of the Nappe Zone Northern Tunisia, and Comparisons with MVT Deposits in the Region. In: In Mineral Deposits of North Africa. Springer International Publishing, pp. 497–525.

Fournier, R.O., 1985. The behavior of silica in hydrothermal solutions. In: Berger, B.R., Bethke, P.M. (Eds.), Geology and Geochemistry of Epithermal Systems, 2, pp. 45–61 (Reviews in Econ. Geol.).

Frizon de Lamotte, D., Saint Bezar, B., Bracène, R., Mercier, E., 2000. The two main steps of the Atlas building and geodynamics of the western Mediterranean. Tectonics 19 (4), 740–761.

Gharbi, M., Ben Ayed, N., Ben Said, E.A., 1981. Essai d interprétation tectonique du champ filonien de Bou-Jaber (Atlas tunisien central): Actes du Premier Congrès national de la terre (Tunis). Tome 1, 393–403.

Grootenboer, J., Schwarcz, H.P., 1969. Experimentally determined sulfur isotope fractionations between sulfide minerals. Earth Planet Sci. Lett. 7, 162–166.

Hanor, J.S., 2000. Barite-celestine geochemistry and environments of formation. In: Alpers, C., Jambor, J., Norstrom, K. (Eds.), Sulphate Minerals. Reviews in Mineralogy and Geochemistry, 40, pp. 193–275.

Jemmali, N., Souissi, F., Vennemann, T., Carranza, E.J.M., 2011a. Genesis of the Jurassic carbonate-hosted Pb-Zn deposits of Jebel Ressas (North-Eastern Tunisia): evidence from mineralogy, petrography and trace metal contents and isotope (O, C, S, Pb) geochemistry. Resour. Geol. 61, 367–383.

Jemmali, N., Souissi, F., Villa, I.M., Vennemann, T., 2011b. Ore genesis of Pb-Zn deposits in the Nappe zone of Northern Tunisia: constraints from Pb-S-C-O isotopic systems. Ore Geol. Rev. 40, 41–53.

Jemmali, N., Souissi, F., Carranza, E.J.M., Vennemann, T.W., 2013a. Sulfur and lead isotopes of Guern Halfaya and Bou Grine deposits (Dome zone: northern Tunisia): Implications for sources of metals and timing of mineralization. Ore Geol. Rev. 54, 17–28.

Jemmali, N., Souissi, F., Carranza, E.J.M., Bouabdellah, M., 2013b. Lead and sulfur isotope constraints on the genesis of the polymetallic mineralization at Oued Maden, Jebel Hallouf and Fedj Hassene carbonate-hosted Pb-Zn (As-Cu-Hg-Sb) deposits, Northern Tunisia. J. Geochem Explor. 132, 6–14.

Jemmali, N., Souissi, F., Carranza, E.J.M., Vennemann, T.W., Bogdanov, K., 2014. Geochemical constraints on the genesis of the Pb-Zn deposit of Jalta (northern Tunisia): Implications for timing of mineralization, sources of metals and relationship to the Neogene volcanism. Chemie der Erde-Geochemistry 74 (4), 601–613.

Jeong, Y.J., Cheong, C.S., Shin, D., Lee, K.S., Jo, H.J., Gautam, M.K., Lee, I., 2012. Regional variations in the lead isotopic composition of galena from southern Korea with implications for the discrimination of lead provenance. J. Asian Earth Sci. 61, 116–127.

Jorgensen, B.B., Isaksen, M.F., Jannasch, H.W., 1992. Bacterial sulfate reduction above 100 degrees Celsius in deep-sea hydrothermal vent sediments. Science 258 (5089), 1756–1758.

Kiyosu, Y., Krouse, H.R., 1990. The role of organic acid in the abiogenic reduction of sulfate and the sulfur isotope effect. Geochem. J. 24 (1), 21–27.

Leach, D.L., 1994. Genesis of the Ozark Mississippi Valley-Type metallogenic province. In: Fontebote, L., Boni, M. (Eds.), Sediment Hosted Zn-Pb Ores. Springer–Verlag, pp. 104–138.

Machel, H.G., Krouse, H.R., Sassen, R., 1995. Products and distinguishing criteria of bacterial and thermochemical sulfate reduction. Appl. Geochem. 10, 373–389.

Maghreb Minerals plc, 2008. Zinc Exploration in North Africa. http://equatorgold.co.uk/finex/downloads/presentations/2008/222.ppt.

Melki, F., Zargouni, F., 1991. Tectonique cassante post jurassique de la mine de Hammam Zriba (Tunisie nord-orientale). Incidences sur la karstification et les concentrations de fluorine, barytine et celestine, d'environnement carbonate. Bull. Soc. Géol. Fr. 162 (5), 851–858.

Morgan, M., Grocott, J., Moody, R., 1998. The structural evolution of the Zaghouan-Ressas structural belt, northern Tunisia. Geol. Soc. London Spec. Publ. 132, 405–422.

Perthuisot, V., 1978. Dynamique et pétrogenèse des extrusions triasiques en Tunisie septentrionale. Theses, Doctorat d'Etat, Ecole Normale supérieure de Paris, Travaux du Laboratoire de Géologie 12, 312 pp.

Rddad, L., Bouhlel, S., 2016. The bou dahar jurassic carbonate-hosted Pb–Zn–Ba deposits (Oriental high atlas, Morocco): fluid-inclusion and C-O-S-Pb isotope studies. Ore Geol. Rev. 72, 1072–1087.

Rhodes, D., Lantos, E.A., Lantos, J.A., Webb, R.J., Owens, D.C., 1984. Pine Point orebodies and their relationship to the stratigraphy structure, dolomitization and karstification of the Middle Devonian Barrier Complex. Econ. Geol. 79, 991–1055.

Souissi, F., Dandurand, J., Fortuné, J., 1997. Thermal and chemical evolution of fluids during fluorite. Miner. Deposita 32, 257–270.

Souissi, F., Sassi, R., Bouhlel, S., Dandurand J-, L., 2007. Fluid inclusion microthermometry and rare earth element distribution in the celestite of the Jebel Doghra ore deposit (Dome zone, Northern Tunisia): towards a new genetic model. Bull. Soc. Géol. Fr. 178 (6), 459–471.

Souissi, F., Souissi, R., Dandurand, J., 2010. The Mississippi Valley-type fluorite ore at Jebel Stah (Zaghouan district, north-eastern Tunisia): contribution of REE and Sr isotope geochemistries to the genetic model. Ore Geol. Rev. 37, 15–30.

Souissi, F., Jemmali, N., Souissi, R., Dandurand, J.L., 2013. REE and isotope (Sr, S, and Pb) geochemistry to constrain the genesis and timing of the F–(Ba–Pb–Zn) ores of the Zaghouan district (NE Tunisia). Ore Geol. Rev. 55, 1–12.

Thibieroz, J., 1974. Hammam Jedidi et Hammam Zriba: Etude géologique et minière de deux gisements stratiformes dans le cadre de la province fluorée tunisienne; l'association des concentrations fluorées aux surfaces d'émersion. 1974. Thèse de 3e cycle univ. Paris VI. 367p.

Thibieroz, J., 1976. Reconstitution chronologique du rôle des surfaces d'émersion dans l histoire du gisement de fluorine de hammam Zriba (région de Zaghouan Tunisie). Mém. H. série soc Géol. Fr. 7, 33–37.

Thode, H.G., Monster, J., 1965. Sulphur isotope geochemistry of petroleum, evaporites and ancient seas. In: Young, A., Galley, J.E. (Eds.), Fluids in Subsurface Environments, 4. Am. Ass. Petrol. Geol, Tulsa, Oklahoma, USA, pp. 367–377.

Zartman, R.E., Doe, B.R., 1981. Plumbotectonics – the model. Tectonophysics 75, 135–162.

De Lamotte, D.F., Leturmy, P., Missenard, Y., Khomsi, S., Ruiz, G., Saddiqi, O., Guillocheau, F., Michard, A., 2009. Mesozoic and Cenozoic vertical movements in the Atlas system (Algeria, Morocco,Tunisia): an overview. Tectonophysics 475 (1), 9–28.